# Fiber optic sensors for precursory acoustic signals detection in rockfall events

**L. Schenato** Research Institute for Geo-Hydrological Protection, National Research Council of Italy, 35127 Padova, Italy
luca.schenato@cnr.it

**L. Palmieri** Department of Information Engineering, University of Padova, 35131 Padova, Italy

**G. Gruca** Department of Physics and Astronomy and LaserLaB, VU Amsterdam, 1081 Amsterdam, The Netherlands

**D. Iannuzzi** Department of Physics and Astronomy and LaserLaB, VU Amsterdam, 1081 Amsterdam, The Netherlands

**G. Marcato** Research Institute for Geo-Hydrological Protection, National Research Council of Italy, 35127 Padova, Italy

**A. Pasuto** Research Institute for Geo-Hydrological Protection, National Research Council of Italy, 35127 Padova, Italy

**A. Galtarossa** Department of Information Engineering, University of Padova, 35131 Padova, Italy

Two fiber optic sensors (FOSs) for detection of precursory acoustic emissions in rockfall events are addressed and experimentally characterized. Both sensors are based on interferometric schemes, with the first one consisting of a fiber coil used as sensing element and the second one exploiting a micro-machined cantilever carved on the top of a ferrule. Preliminary comparisons with standard piezo-electric transducers shows the viability of such FOSs for acoustic emission monitoring in rock masses.
[DOI: http://dx.doi.org/10.2971/jeos.2012.12048]

**Keywords:** Fiber optic sensor, acoustic emission, rock monitoring, interferometry

## 1 INTRODUCTION

Collapses of rock masses represent a major source of hazard in mountain areas, being the cause of rapid landslides. Differently from landslides occurring in earth or debris, which are usually surveyed by directed inspection of their surface, rockslides offer few, if any, visible signs. Furthermore rockslides apparently occur all of a sudden [1], making the application of early warning procedures very urgent. Rockslides are associated to processes of stress accumulation in unstable rocks, during which part of the accumulated energy is released in small internal cracks [2]. These cracks generate acoustic emissions (AE) that can, therefore, be used as precursory signals, through which unstable rocks could be monitored. In particular, geological models and experiments have suggested that AE in the range $20 \div 100$ kHz (the lower limit being set mainly to greatly limit anthropic noise) are the most indicate to be monitored for that purpose [3, 4].

Unfortunately, the application of traditional AE sensors, such as accelerometers and piezoelectric transducers, finds serious practical limitations due to the faintness of these AEs and the hostility of typical mountain environment (with severe temperature, frequent lightning and ice storms, heavy rains and arduous access). Furthermore, the conventional method consists, basically, in the bare counting of events or of the number of times the AE signal crosses an a-priori defined detection threshold (the so called *ring down count*): the temporal distribution of such parameters has been considered enough, so far, to the aim of monitoring the rock stability [5, 6].

With this respect, FOSs may fill the gap, providing a reliable solution and potentially offering the following features: more robustness to electromagnetic interference, smaller form factor, multiplexing capability, longer distance range (which lead to easiness of installation), higher sensitivity. To explore this possibility, in this work we analyze two fiber-based optical sensors for AE detection in rock masses. Both sensors are interferometric. The first one uses a 100-m-long fiber coil as the sensing arm of an heterodyne Mach-Zehnder interferometer [7]. The second one is a Fabry-Perot micro-cavity obtained by carving a cantilever on the top of a fiber-bearing ferrule, according to the methodology proposed in [8].

This paper extends the results presented in [9, 10] and is organized as follows: in the Section 2, the two sensors are briefly introduced; their experimental characterization is described in Section 3 where their performances are compared with a standard piezo-electric transducer (PZT). Finally, conclusions are drawn in Section 4: results, while not yet conclusive, confirm that FOSs may represent a viable solution for AEs detection in unstable rock masses monitoring.

Received June 29, 2012; revised ms. received October 29, 2012; published November 18, 2012 ISSN 1990-2573

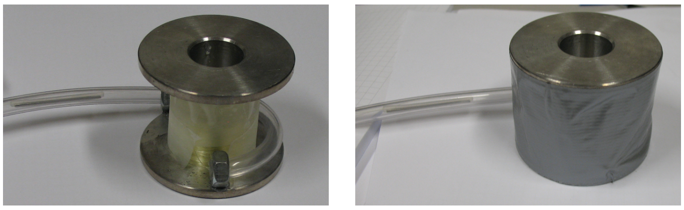

(a) (b)

FIG. 1 The fiber coil sensor: (a) the bare rugged sensor; (b) after it has been acoustically insulated from the environment by means of a layer of acoustic absorbing material and covered by tape.

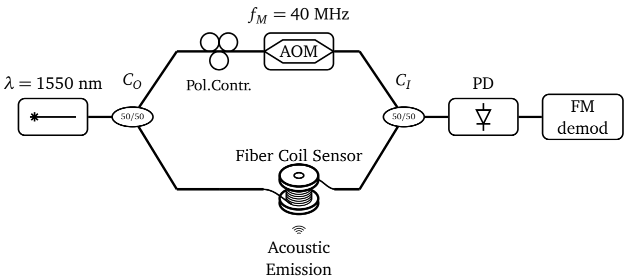


FIG. 2 Setup of the sensing scheme for FCS: the light source is a high-coherence DFB laser at 1550 nm; AOM: acousto-optic modulator at 40 MHz; Co and C1: optical coupler; PD: photodiode; FM demod: double balanced quadrature FM detector board.

## 2 THE FIBER OPTIC SENSORS

The fiber optic AE sensors addressed here are interferometric devices. The first sensor is shown in Figure 1. It consists in approximately 100 m of G.657 optical fiber, tightly wound on an aluminum flanged hollow mandrel (inner diameter 30 mm, height 42 mm). A layer of acoustic absorbing material is applied to insulate the mandrel from the environment. The mandrel can be fastened to the rock by means of a 4-cm-long M10 screw, which acts, also, as the main acoustic coupling element between the rock and the sensor.

This fiber coil sensor (FCS) is inserted in the sensing arm of a heterodyne fiber Mach-Zehnder interferometer, represented in Figure 2; the interferometer is interrogated by a high-coherence laser with $\lambda = 1550$ nm. The acousto-optic modulator in the reference arm downshifts the laser frequency by 40 MHz, thus enabling heterodyne detection at the receiver. The use of an heterodyne scheme improves the performance of the setup with respect to the standard homodyne technique: in fact, it allows (i) to reduce the amount of $1/f$ noise, (ii) to avoid the need of an accurate control of laser wavelength (and related thermal drift), and (iii) to relax constraints posed by polarization sensitivity [11]. On the other side, however, it makes the detection more complicated, because a frequency demodulator is needed to retrieve information about AE which is encoded on the phase of the detected signal.

The second sensor, shown in Figure 3, is made of a micro cantilever carved on the top of a cylindrical silica ferrule [8]. The cantilever lays parallel to the ferrule top along its diameter with only one end attached to the ferrule: in this way the cantilever is free to oscillate under external perturbations. The ferrule houses a standard single mode fiber, and the gap between the cantilever and the fiber end face behaves as a resonating vibration-sensitive Fabry-Perot cavity. The ferrule is about 10 mm long and has a diameter of 2 mm; the cantilever, made of Duran, is about 1.25 mm long, 35 $\mu$m thick and 220 $\mu$m wide; the gap between the cantilever and the fiber is about 100 $\mu$m. In order to increase the reflectivity of the cavity, the upper face of the cantilever is coated by a thin layer of gold. These parameters, along with the Young modulus and density of Duran, allow to calculate the first nominal mechanical resonance by means of the Euler-Bernoulli equation [12]; accordingly:

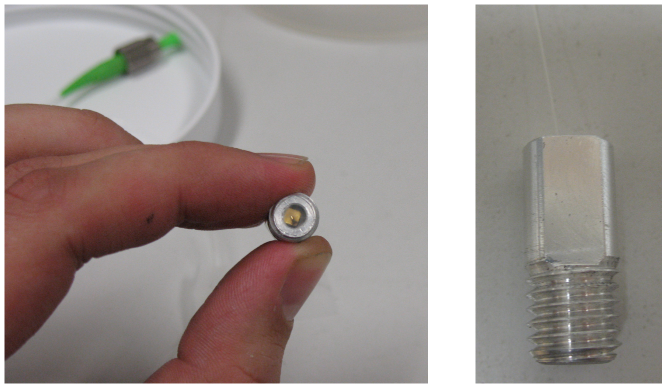

(a) (b)

FIG. 3 The ferrule top cantilever sensor: (a) front view; (b) side view.

$$\nu = \frac{\kappa^2}{2\pi}\sqrt{\frac{E}{\rho}\frac{w\,t^3}{12}\frac{1}{wtL^4}} \sim 19.4 \text{ kHz}, \tag{1}$$

where $\kappa = 1.875$, $E = 64$ Gpa and $\rho$=2.23 g/cm$^3$ are, respectively, Young Modulus and density of Duran and $w$, $t$ and $L$ are the width, thickness and length of the cantilever, respectively. The measured mechanical resonance is 12.5 kHz and differs significantly from the calculated one: this is actually a common problem that afflicts also commercial atomic-force-microscope probe where resonance frequency is typically within $\pm$50% from its nominal value. Ultimately, this can be imputed to several reasons: a not perfect rectangular shape, a not uniform thickness of the cantilever, presence of the thin gold layer that coats the upper cantilever face, presence of glue which fills in the bore hole on the cantilever. Finally, the Q-factor of the cantilever has been roughly estimated in 400, by measuring experimentally the relaxation time of the damped harmonic oscillation signal from the sensor [13].

A 20-mm-long M10 bored bolt housed this ferrule top cantilever sensor (FTC), while providing both protection and a suitable mean of mechanical and acoustic coupling to the rock.

The reflectivity of the FP cavity, which is probed by a low-coherence laser tuned at the quadrature point of the cavity, changes accordingly to the AEs induced vibrations, and that information is decoded with the setup shown in Figure 4.

## 3 EXPERIMENTS

Acoustic coupling and impedance matching play a crucial role in the performance of AE sensors [14]; therefore, in order to get realistic testing conditions, we have tested the sensors on a block of Montemerlo Classic Gray Trachyte ($50 \times 50 \times 15$ cm in size, about 100 kg in weight). The FOSs were screwed in

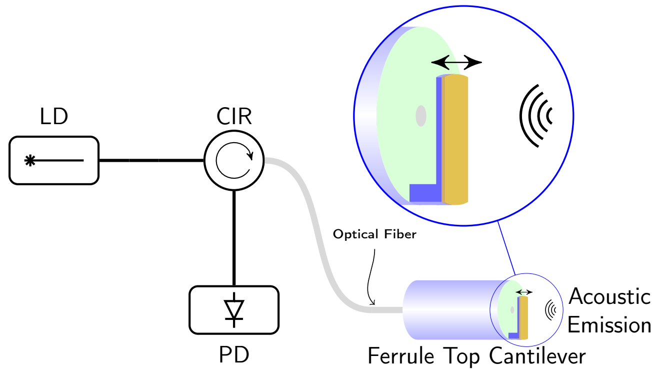


FIG. 4 Setup of the sensing scheme for FTC: the light source is a low-coherence laser (LD: laser diode) at the quadrature wavelength of the cavity; CIR: optical circulator; PD: photodiode.

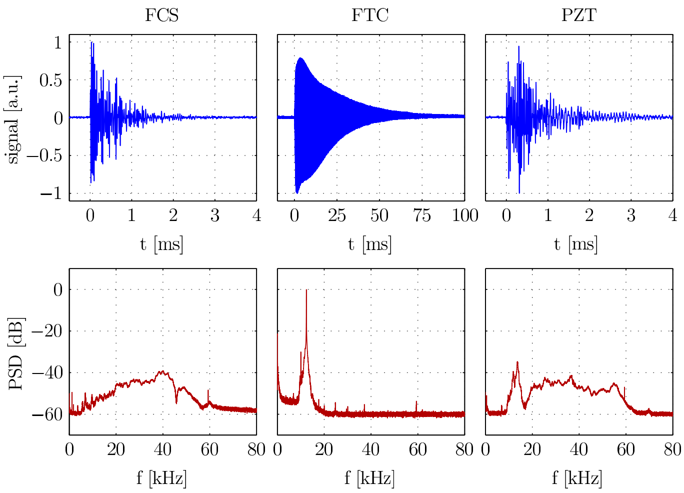


FIG. 5 Typical signals (top row) and corresponding PSDs (bottom row) recorded by the three sensors (FCS, fiber coil sensor; FTC, ferrule-top cantilever; PZT, piezo-electric transducer).

an internally threaded anchor, chemically glued in a hole at the center of one of the block's 50 $\times$ 50 cm faces. For convenience, the block was simply supported at 4 points near the corners of the drilled face; in that way, the sensor under test was screwed in the bottom face of the block, with the top face left clear for the excitation of AEs in different positions. During the tests, an amplified PZT (VS30-SIC-46dB from Vallen Systeme GmbH, 46 dB of electrical amplification) have been used to compare its performances with those of the FOSs. Electrical signals from PZT, FTC photodiode and FCS demodulation board are eventually recorded by a digital storage oscilloscope.

Acoustic emissions have been generated in a repeatable way by the impact of a 5-mm-diameter steel ball dropped along a steep slide, placed on the top of the block [15]. Repeatability of this method of excitation has been tested extensively and it is within 10%; moreover, it has been found that direction of impact of the ball has a negligible effect on the recorded signal.

Upper part of Figure 5 shows, for each of the three sensors (the two FOSs and the PZT), a sample signal recorded when the ball is dropped at the center of the upper face of the trachyte block. Right below in Figure 5, the corresponding power

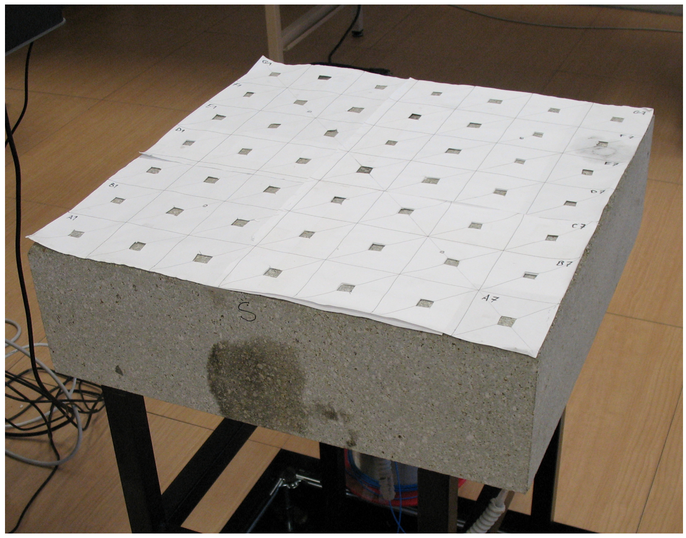

FIG. 6 Upper face of the trachyte block with the uniform grid according to which the ball has been dropped to test the responsivity of the sensors.

spectral densities (PSD) are represented. It can be noted that, amongst the three sensors, the PZT has the most flat spectral response. As expected, the spectral response of the FTC is dominated by a peak centered at 12.5 kHz, the resonance frequency of the cantilever. Correspondingly, the time evolution of the signal recorded by the FTC is basically a damped oscillation. On the contrary, the signals recorded by the FCS and the PZT are close to the actual AE. Even though the FTC can provide very little information about the spectral content of the AE, this is not at all a limitation, since as noted in the introduction section the bare detection and counting of AE events, enabled by the FTC, is the standard methodology for the present geological application. Rather, the prolonged temporal damping of the signal from FTC, contributes in enhancing the sensitivity, although this comes at the expense of a reduced capability of resolving in time two consecutive AEs.

To compare the three sensors, several tests have been performed by dropping the ball at different positions on an uniform $7 \times 7$ grid, drawn on the top 50 $\times$ 50 cm face of the block, as in Figure 6.

For each dropping, a signal, $y(t)$, has been recorded and the "acoustic energy" over an arbitrary window $T$ defined as $Y(t) = \int_t^{t+T} y^2(\tau)\,d\tau$ has been calculated. The window length $T$ has been chosen as the average length of the event, as recorded by the specific sensor. Actually, using a window longer than the event would be pointless, because it would just includes more noise in the integral. Therefore, we have set $T = 5$ ms for FCS and PZT, whereas for the FTC, owing to its damping behavior, we have set $T = 100$ ms. As stated above, this longer integration window results in a improved sensitivity but in a more realistic scenario where a sequence of AEs may occur, increasing $T$ reduces temporal resolution, as well. Then we have defined the recorded intensity of the AE as $\max_t\{Y(t)\}$.

The results of these tests have been plotted in the three uppermost graphs of Figure 7, where we have represented the intensities detected by each sensor with respect to the different dropping positions on the grid. To compare results, intensi-

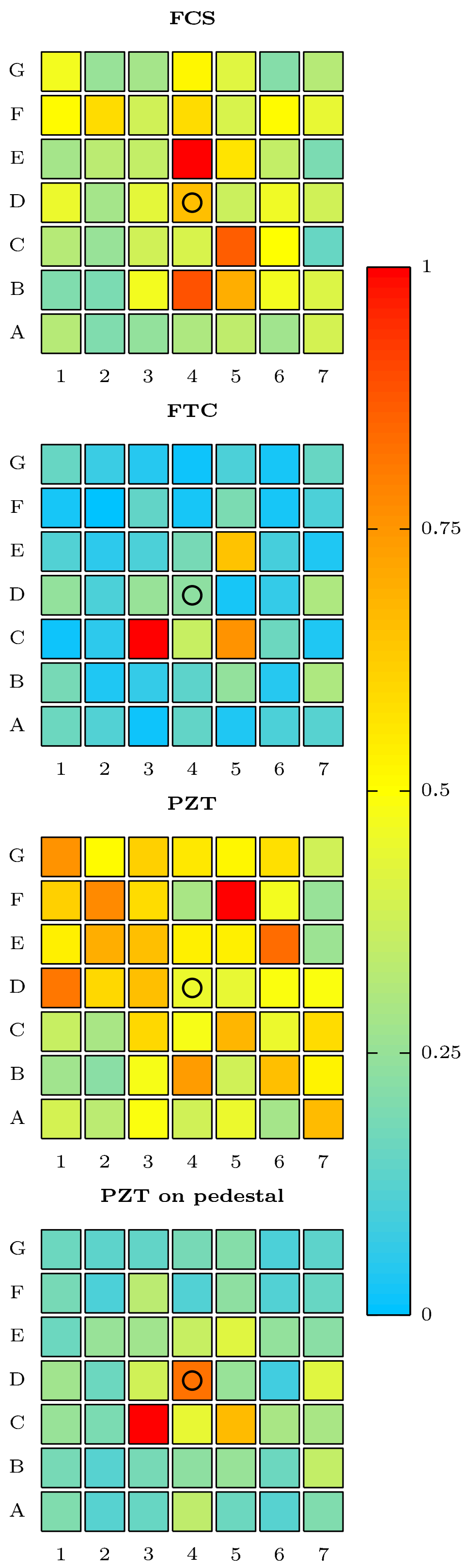


FIG. 7 Normalized intensities recorded by the sensors as a function of the position of impact (FCS, fiber coil sensor; FTC, ferrule-top cantilever; PZT, piezo-electric transducer; empty circles indicate sensor position).

ties have been normalized for each sensor independently, with respect to their maximum on the grid: as expected, the sensors mostly show higher intensities when the ball is dropped closer to the center, where sensors were screwed. Nevertheless, this correspondence is not perfect, likely because of inhomogeneities in the rock block. Moreover, it can be noticed that the more marked dependency on the excitation position is exhibited by the FTC, followed by the FCS, and then, by the PZT. We impute these differences mainly to a different sensitivity of sensors to surface waves, induced by the impact. Actually, while the PZT is coupled to the rock only by means of its flat surface, the FTC is totally inserted inside the rock and therefore it is more sensitive to volume waves. On the other side, the FCS is acoustically coupled both through the screw, and through one of the mandrel flanges that in in contact with the flat block surface. To support this argumentation, the test has been repeated by installing the PZT on a pedestal, made of a long flat-head bolt directly screwed into the block, as it happens to the FOSs. In this way, we are confident to reduce the surface coupling, and hence we expected the PZT to become more sensitive to volume waves. Results, reported in the lowermost graph of Figure 7, show a marked increase of the dependency on the excitation position, in agreement with our hypothesis. We remark that the intrinsic insensitivity to surface waves is a desirable feature, because noise sources (e.g. anthropic activities and meteors) acting outside real rock masses are most likely to induce surface waves, rather than volume ones.

About absolute performances, the FCS is the least sensitive of the three sensors: with respect to FCS, the peak intensities of FTC and PZT are about 30 dB and 50 dB higher, respectively. Notice, however, that both FTC and PZT include at the receiver an electrical amplification of 20 dB and 46 dB, respectively; differently, electrical amplification is not exploited in the FCS. Taking that gain amplification into account, the most sensitive sensor is the FTC, although we recall that this performance comes at the expense of a twenty-fold reduction of temporal resolution. Noise performances are comparable, since the three sensors have an SNR of about 30 dB. Analogous results have been obtained by changing the position at which sensors were screwed at the bottom face of the trachyte block.

## 4 CONCLUSIONS

In this paper some preliminary experimental analyses aimed at exploring the applicability of FOSs to the monitoring of unstable rock masses have been reported. Two different interferometric sensors have been considered and compared with a standard PZT: the first sensor is based on a fiber coil, FCS, while the second one is based on a ferrule top cantilever, FTC The PZT outperforms both FOSs in term of sensitivity, yet it should be remarked that this is mainly due to its internal 46-dB electrical amplification. By taking into account the differences in electrical amplification, the FTC is the most sensitive sensor, although FTC is also the one with the least temporal resolution. Experimental results suggest also that FOSs (FTC, in particular) could be intrinsically more sensitive to volumes waves, whereas PZT appears to be more sensitive to surface waves. To the aim of rock mass monitoring, this characteristic of the FOSs is highly desirable, because surface waves are more easily triggered by environmental noise. While further developments and investigations are needed, this preliminary analysis has shown that FOSs represent a viable approach to the monitoring of unstable rock masses.

## 5 ACKNOWLEDGEMENTS

The research was supported by Fondazione Cassa di Risparmio di Padova e Rovigo under the project SMILAND, by the European Research Council under the European Community's Seventh Framework Programme (FP7/ 2007-2013)/ERC grant agreement 201739, by the European COST Action TD1001 "OFSeSa", and by the Stichting voor Fundamenteel Onderzoek der Materie (FOM) under the Valorization grant number 11VAL11C.
Logistic support by Lucio Baseggio is acknowledged.

## References

[1] T. H. Erismann and G. Abele (eds.), *Dynamics of Rockslides and Rockfalls* (Springer, New York, 2001).

[2] D. Amitrano, "Rupture by damage accumulation in rocks", Int. J. Fracture **139**, 369–381 (2006).

[3] G. Manthei, J. Eisenblätter, and T. Spies, *Acoustic Emission in Rock Mechanics Studies in Acoustic Emission - Beyond the Millennium* (Elsevier, London, 2000).

[4] N. Rosser, M. Lim, D. Petley, S. Dunning, and R. Allison, "Patterns of precursory rockfall prior to slope failure," J. Geophys. Res. **112**, F04014 (2007).

[5] A. Lavrov, "The Kaiser effect in rocks: principles and stress estimation techniques," Int. J. Rock Mech. Min. **40**, 151–171 (2003).

[6] N. Dixon, R. Hill, and J. Kavanagh, "Acoustic emission monitoring of slope instability: development of an active waveguide system," P. I. Civil. Eng. - Geotec. **156**, 83–95 (2003).

[7] J. H. Cole, C. Kirkendall, A. Dandridge, G. Cogdell, and T. G. Giallorenzi, "Twenty-five years of interferometric fiber optic acoustic sensors at the Naval Research Laboratory," Washington Academy of Sciences, 40–57 (2004).

[8] G. Gruca, S. de Man, M. Slaman, J. H. Rector, and D. Iannuzzi, "Ferrule-top micromachined devices: design, fabrication, performance," Meas. Sci. Technol. **21**, 094033 (2010).

[9] L. Schenato, L. Palmieri, F. Chiarello, G. Marcato, G. Gruca, T. van de Watering, D. Iannuzzi, A. Pasuto, and A. Galtarossa, "Experimental analysis of fiber optic sensor for detection of precursory acoustic signals in rockfall events," in *Proceedings to Fotonica 2012, 14$^{th}$ Convegno Nazionale delle Tecnologie Fotoniche* (AEIT, Firenze, 2012).

[10] L. Schenato, L. Palmieri, L. Vianello, G. Marcato, G. Gruca, T. van de Watering, D. Iannuzzi, A. Pasuto, and A. Galtarossa, "Analysis of fiber optic sensor application to precursory acoustic signals detection in rockfall events," in *Proceedings to 22nd International Conference on Optical Fiber Sensors (OFS-22)* (SPIE, Beijing, 2012).

[11] K. Kageyama, H. Murayama, K. Uzawa, I. Ohsawa, M. Kanai, Y. Akematsu, K. Nagata, and T. Ogawa, "Doppler effect in flexible and expandable light waveguide and development of new fiber-optic vibration/acoustic sensor," IEEE/OSA J. Lightw. Technol. **24**, 1768–1775 (2006).

[12] S. M. Han, H. Benaroya, and T. Wei, "Dynamics of Transversely Vibrating Beams using Four Engineering Theories," J. Sound Vib. **225**, 935–988 (1999).

[13] F. R. Blom, S. Bouwstra, M. Elwenspoek, and J. H. J. Fluitman, "Dependence of the quality factor of micromachined silicon beam resonators on pressure and geometry," J. Vac. Sci. Technol. B **10**, 19–26 (1992).

[14] J. Eisenblätter, C. U. Grosse, S. Köppel, J. H. Kurz, E. N. Landis, L. M. Linzer, G. Manthei, M. Ohtsu, B. Schechinger, B. Schechinger, T. Shiotani, and T. Vogel, *Acoustic Emission Testing* (Springer, New York, 2008).

[15] N. Carino, "The impact-echo method: an overview", in *Proceedings of the 2001 Structures Congress & Exposition*, P. C. C. Editor, ed. (American Society of Civil Engineers, Washington D.C., 2001).